



## The study of ethanol and water vapour permeation process through alginate membranes modified by magnetic powders

Gabriela Dudek<sup>a,\*</sup>, Małgorzata Gnus<sup>a</sup>, Roman Turczyn<sup>a</sup>, Krystyna Konieczny<sup>b</sup>

<sup>a</sup>Silesian University of Technology, Faculty of Chemistry, Strzody 9, 44-100 Gliwice, Poland, email: gmdudek@polsl.pl

<sup>b</sup>Silesian University of Technology, Institute of Water and Wastewater Engineering, Konarskiego 18, 44-100 Gliwice, Poland

Received 3 April 2016; Accepted 30 June 2016

### ABSTRACT

This paper presents a study of novel hybrid membranes consisting of sodium alginate as a polymer matrix and magnetite and two cross-linking agents, that is, orthophosphoric acid and  $\text{Ca}^{2+}$  ions. Ethanol/water separation parameters were determined using the vapour permeation process. The permeate parameters were estimated on the basis of weight loss of the measuring cell over time using an analytical balance. The results have shown the influence of magnetite particles content in the alginate matrix and the effect of cross-linking agents on ethanol/water separation properties. Comparing permeation coefficients of both types of discussed membranes more advantageous separation properties for the membranes cross-linked with orthophosphoric acid were observed. The best ideal selectivity (55.54) was recorded for membranes with iron oxide content between 5 and 10 w/w%. For  $\text{Ca}^{2+}$  ions cross-linked membranes, the highest ideal selectivity coefficient can be obtained at 15–20 w/w% magnetite content (32.18).

*Keywords:* Sodium alginate; Magnetite; Hybrid membranes; Transport properties; Vapour permeation

### 1. Introduction

Over the last 20 years, the growing interest in industrial application of liquid mixtures separation using a vapour permeation process has been observed. For instance, LURGI GmbH and UBE metal and chemical industries applied the vapour permeation process in separation of the water/ethanol mixture [1]. The vapour permeation process is also gaining popularity as a method of recovering organic compounds vapours from the air. An example would be separation of dimethylpropylamine from polluted air, the product of which can be used as a catalyst for curing of synthetic resins [2]. In the field of vapour permeation, the scientific effort is primarily focused on studying separation properties of polymeric materials. Equal importance is given to optimisation of the separation process including improvements in membrane module construction methods [2–6].

The development of new, selective membrane materials still generates a great interest. In the last years, application of biopolymers has increased significantly due to their excellent biocompatibility, biodegradability, high hydrophilicity, inexpensiveness and non-toxicity. The most commonly used biopolymers are chitosan and alginate [7–21]. Alginate is a typical hydrophilic polysaccharide, component of the cell walls of algae. It consists of a linear copolymer composed of two monomer units, 1,4-linked  $\beta$ -D-mannuronic acid and  $\alpha$ -L-guluronic acid, in varying proportions. Sodium alginate (NaAlg) has exhibited many intrinsic properties, such as high hydrophilicity and good film-formation characteristics. Thus, it is considered as a prospective membrane material applicable for membrane separation technology, adsorption of dyes and metal ions [7–10].

One useful strategy of improving separation efficiency of polymeric membranes is formation of hybrid materials through the incorporation of various inorganic materials, typically oxides or metal nanoparticles, into the polymer

\* Corresponding author.

Presented at the conference on Membranes and Membrane Processes in Environmental Protection (MEMPEP 2016), Zakopane, Poland, 15–19 June 2016.

matrix. These hybrid membranes benefit from the selectivity of active components and the simplicity of polymeric membrane processing. The effectiveness of this type of membranes depends mainly on the interaction between components and penetrants, their compatibility and homogeneous dispersion of inorganic component into the polymer matrix [11–17]. In our previous research [18–21], chitosan membranes with varied dose of iron oxide nanoparticles in the process of ethanol dehydration were tested. The results have shown that the addition of magnetite particles to the chitosan matrix created additional free volumes in polymers and, in consequence, offered space for water molecules to permeate easily through the membranes.

In this paper, the differences in transport properties of alginate membranes filled with various amounts of iron oxide nanoparticles ( $\text{Fe}_3\text{O}_4$ ) are discussed. The tests were conducted with alginate membranes cross-linked with orthophosphoric acid and  $\text{Ca}^{+2}$  ions. Based on the experimental vapour permeation of water and ethanol measured using the permeation vessel method, the transport characteristics and ideal separation coefficients were evaluated.

## 2. Materials and methods

### 2.1. Preparation of cross-linked alginate magnetic membrane

A 1.5% alginate solution was prepared by dissolving sodium alginate powder in water. The solution was mixed with an appropriate portion of magnetite nanoparticles (0%, 5%, 10%, 15%, 20%, 25%) prepared beforehand using a precipitation method described in [13]. The ultrasonic bath was used to disperse magnetite nanoparticles and de-aerate the solution. The homogeneous solution was then cast on a glass plate and dried at  $40^\circ\text{C}$  for 24 h. Next, the membrane was cross-linked by immersing alginate membranes at room temperature in the appropriate cross-linker solution, that is, 3.5 v/v% orthophosphoric acid solution or 2.5 w/w% calcium chloride solution. The obtained membrane was removed from the glass plate, washed with ethanol and dried.

### 2.2. Experimental setup

In order to study the vapour permeation process of water and ethanol through alginate membranes, the permeation vessel method was applied. A measuring vessel was a top-opened, aluminium, cylindrical pot illustrated in Fig. 1. The liquid was poured only to fill two-thirds of the vessel, and a membrane firmly covering the top of container was fixed by an aluminium ring. To prevent absorption of vapours from the environment onto the studied membranes, the measuring vessel was kept in a desiccator (Fig. 2). In addition, the desiccator was flushed with dried air (desiccant  $\text{CaSO}_4$ , flow rate  $50 \text{ cm}^3 \text{ min}^{-1}$ ). The weight loss of the vessel, separately for water and ethanol (99.8 v/v%), was measured at fixed time intervals at room temperature (r.t.). The thickness of all membranes was measured using a waterproof precise coating thickness gauge (MG-401 ELMETRON) and was estimated as a mean value of at least 10 measurements taken in different locations.

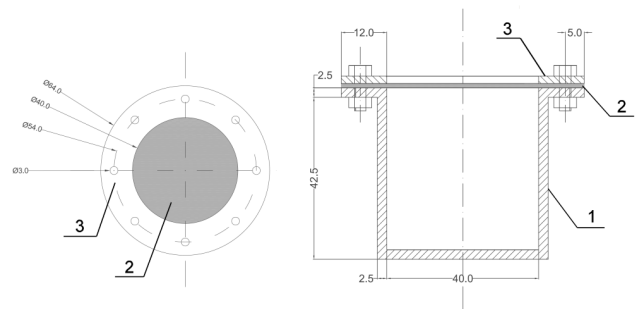


Fig. 1. Schematic diagram of the measuring vessel.

Note: 1 – cylindrical measuring cell, 2 – membrane, and 3 – fixing aluminium ring.

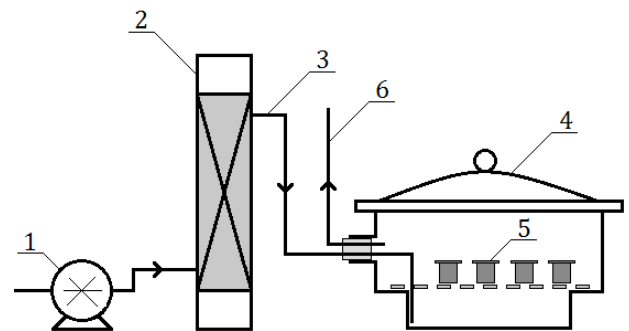


Fig. 2. Permeation apparatus.

Note: 1 – pump, 2 – desiccant cartridge ( $\text{CaSO}_4$ ), 3 – air inlet, 4 – desiccator, 5 – measuring vessels, and 6 – air outlet.

### 2.3. Evaluation of the permeation process parameters

The basic law of a phenomenological, parabolic diffusion through a slab membrane of unit cross-section is defined by Fick's law [22]:

$$J = -D \frac{\partial c}{\partial x} \quad (1)$$

where  $J$  is the diffusion flux;  $c$  is concentration of the diffusing species;  $D$  is a diffusion coefficient; and  $x$  is membrane cross-section. Crank and Park [23] reviewed the most useful experimental techniques for measuring the diffusion coefficient. The most fundamental formula to quantify the average diffusion coefficient  $\bar{D}$  valid in stationary permeation conditions is as follows:

$$\bar{D} (\text{cm}^2 \cdot \text{s}^{-1}) = \frac{J_s \cdot l}{\Delta c_0} \quad (2)$$

where  $J_s$  is a diffusive mass flux in a stationary state;  $l$  is membrane thickness; and  $\Delta c_0$  can be obtained from an intercept of the asymptote to the stationary permeation curve with the  $Q^s(l, t)$  axis (total flow of penetrant) (Fig. 3).

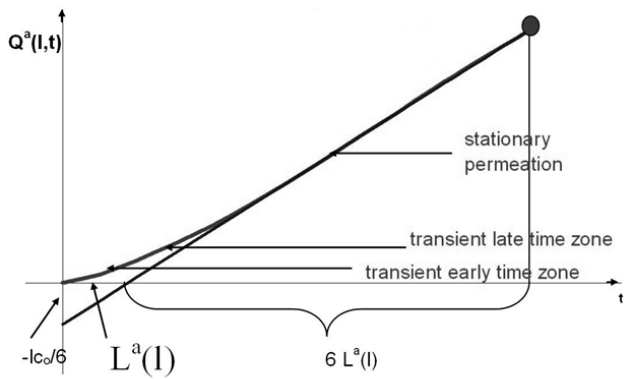


Fig. 3. Schematic view of downstream absorption permeation curve.

By comparing  $\bar{D}$  with the value of diffusion coefficient  $D_L$  calculated from the downstream absorption time lag [24,25] according to the following equation:

$$D_L (\text{cm}^2/\text{s}) = \frac{l^2}{6L^a(l)} \quad (3)$$

we can get some insight into the nature of the transport process in question. Namely if  $\bar{D} = D_L$ , the diffusion is estimated to be an “ideal Fickian” unless there are some hidden processes, like a drift, which are beyond the reach of this simple protocol [26].

The permeability coefficient can give insight into how fast the penetrant can pass through the membrane and be determined as follows:

$$P = \frac{J_s \cdot l}{\Delta p} \quad (4)$$

where  $P$  is the permeability coefficient;  $l$  is membrane thickness;  $\Delta p$  is the difference of gas pressure at both sides of the membrane; and  $J_s$  is the diffusive mass flux in a stationary state.

Table 1

Test results: transport parameters of water and ethanol for orthophosphoric acid cross-linked alginate magnetite membranes

	Magnetite content, w/w%					
	Water					
	0	5	10	15	20	25
Diffusion coefficient $D_L \cdot 10^{10}$ , $\text{cm}^2 \cdot \text{s}^{-1}$	5.10 ± 0.82	2.78 ± 0.35	2.54 ± 0.17	2.67 ± 0.53	2.26 ± 0.12	2.27 ± 0.21
Flux $J$ , $\text{g} \cdot \text{m}^{-2} \cdot \text{h}^{-1}$	116.42 ± 2.60	137.00 ± 2.42	137.87 ± 3.12	140.01 ± 6.89	107.22 ± 2.28	109.56 ± 3.10
Permeation coefficient $P \cdot 10^{14}$ , Barrer	108.63 ± 5.02	142.06 ± 8.14	133.10 ± 6.53	120.15 ± 6.15	101.93 ± 5.83	93.98 ± 3.11
Solubility coefficient $S \cdot 10^4$ , $\text{g} \cdot \text{cm}^{-3} \cdot \text{Pa}^{-1}$	21.3 ± 0.35	51.1 ± 0.61	52.4 ± 0.38	45.0 ± 0.92	45.1 ± 0.22	41.4 ± 0.42
	Ethanol					
Diffusion coefficient $D_L \cdot 10^{10}$ , $\text{cm}^2 \cdot \text{s}^{-1}$	3.57 ± 0.17	2.61 ± 0.35	2.95 ± 0.18	2.63 ± 0.21	2.48 ± 0.34	2.06 ± 0.25
Flux $J$ , $\text{g} \cdot \text{m}^{-2} \cdot \text{h}^{-1}$	7.31 ± 0.14	7.02 ± 0.23	7.56 ± 0.24	7.42 ± 0.13	7.81 ± 0.25	7.25 ± 0.17
Permeation coefficient $P \cdot 10^{14}$ , Barrer	2.53 ± 0.11	2.56 ± 0.18	2.42 ± 0.18	2.55 ± 0.17	2.58 ± 0.16	2.41 ± 0.18
Solubility coefficient $S \cdot 10^4$ , $\text{g} \cdot \text{cm}^{-3} \cdot \text{Pa}^{-1}$	0.71 ± 0.02	0.98 ± 0.03	0.82 ± 0.06	0.97 ± 0.08	1.04 ± 0.12	1.17 ± 0.16
Ideal selectivity $P_{\text{H}_2\text{O}}/P_{\text{EtOH}}$	42.86 ± 1.89	55.54 ± 2.28	55.02 ± 2.41	47.10 ± 2.06	39.52 ± 2.18	38.99 ± 1.12

Diffusive mass flux is defined as follows:

$$J_s = \frac{Q_{STP}}{A} \quad (5)$$

where  $Q_{STP}$  is the flow rate at standard condition, and  $A$  is the active area of membrane.

The solubility coefficient is the equilibrium parameter, and it measures the extent to which the penetrant is sorbed. This parameter is calculated from the following relation:

$$S = \frac{P}{D} \quad (6)$$

where  $S$  is the solubility coefficient;  $P$  and  $D$  are as defined above.

Ideal selectivity coefficient  $\alpha_{ij}$  is defined as a ratio of permeation of gases and for constant membrane thickness  $l$  can be calculated as a ratio of given permeability coefficients [27]:

$$\alpha_{ij} = \frac{P_i}{P_j} \quad (7)$$

### 3. Results and discussion

#### 3.1. Ethanol/water separation through orthophosphoric acid cross-linked magnetite alginate membranes

Table 1 presents the results from the tests conducted during ethanol and water separation through orthophosphoric acid cross-linked magnetite alginate membranes.

The results have shown that the diffusion coefficient ( $D_L$ ) was similar for both water and ethanol permeating through orthophosphoric acid cross-linked alginate magnetite membranes. For pristine alginate membrane, the diffusion coefficients for water and ethanol were equal to  $5.1 \cdot 10^{-10}$  and  $3.6 \cdot 10^{-10} \text{ cm}^2 \cdot \text{s}^{-1}$ ,

respectively. The addition of iron oxide nanoparticles into the alginate matrix decreased the diffusion coefficient of both components to about  $2.5 \cdot 10^{-10} \text{ cm}^2 \cdot \text{s}^{-1}$ . However, the solubility coefficients of water were two orders larger than corresponding coefficients for ethanol. In the case of alginate membranes enhanced with magnetite, the solubility coefficients of two investigated components were substantially larger in comparison with pristine membranes. The water solubility coefficient was the highest at 10 w/w% iron oxide particles content. Furthermore, the larger iron oxide content, the lower solubility coefficient was obtained. In consequence, the highest permeation coefficient levels have been observed for alginate membranes with 5 and 10 w/w% magnetite content. This phenomenon can be explained by the fact that the addition of magnetite nanoparticles to alginate matrix created extra free volumes in polymer and in consequence offered space for water molecules to permeate easily through the membranes [16,17]. Due to aggregation of ferroferric oxide particles onto membranes with magnetite content above 10 w/w% the observed permeation coefficients decreased.

In the case of ethanol, the solubility coefficient has a tendency to increase together with higher magnetite content in the alginate matrix. As a result, the highest value of permeation coefficient was obtained for larger content of iron oxide nanoparticles. In view of hydrophobic character of polar organic solvents like ethanol [28,29], the addition of hydrophilic magnetite nanoparticles, there is no such influence on hydrophobic head groups of ethanol molecules as on hydrophilic water molecules, so obtained permeation coefficients were higher for water than for ethanol.

The permeation coefficients of water and ethanol expressed as ideal selectivity coefficient have shown that the most effective separation between ethanol and water can be obtained using membranes with 5 and 10 w/w% magnetite content, which corresponds to 55.54 and 55.02, respectively. In this case, the difference between water and ethanol permeation coefficients was the greatest, which allows for the best separation between ethanol and water.

### 3.2. Ethanol/water separation through $\text{Ca}^{2+}$ cross-linked magnetite alginate membranes

Results of the vapour permeability measurements through the  $\text{Ca}^{2+}$  cross-linked alginate membranes filled with iron oxide nanoparticles ( $\text{Fe}_3\text{O}_4$ ) are presented in Table 2.

The test results for pristine alginate membranes cross-linked with  $\text{Ca}^{2+}$  ions have shown that diffusion coefficients in water were higher than those for ethanol. Addition of iron oxide nanoparticles into the polymer matrix inverted the relationship between water and ethanol diffusion coefficients. The diffusion coefficient of water decreased after addition of iron oxide nanoparticles and gradually lowered with higher magnetite loading. To the contrary, in tests with ethanol the diffusion coefficient increased with higher content of magnetite. Dissimilar behaviour was demonstrated by solubility coefficients. Iron oxide nanoparticles loading has caused an increase in solubility coefficients of water from  $1.54 \cdot 10^{-4}$  to  $5.49 \cdot 10^{-4} \text{ g} \cdot \text{cm}^{-3} \cdot \text{Pa}^{-1}$  for pristine and 25 w/w% magnetite-loaded alginate membranes, respectively. In contrast, the solubility coefficient of hydrophobic ethanol molecules decreased from  $0.11 \cdot 10^{-4}$  to  $0.04 \cdot 10^{-4} \text{ g} \cdot \text{cm}^{-3} \cdot \text{Pa}^{-1}$  for pristine and 25 w/w% magnetite-loaded alginate membranes, respectively. In consequence, the highest value of permeation coefficient has been observed for alginate membranes with the maximum tested load of iron oxide nanoparticles. When comparing permeation coefficients of water and ethanol, we can notice two orders of magnitude difference, as it was the case in alginate membranes cross-linked with orthophosphoric acid. As presented in Table 2, ideal selectivity coefficient results have indicated possibility of effective separation of water and ethanol using  $\text{Ca}^{2+}$  cross-linked alginate magnetite membranes. The most favourable separation has been demonstrated for membranes with 15 and 20 w/w% ferroferric oxide nanoparticles content, which corresponds to ideal selectivity coefficients equal to 32.18 and 30.40, respectively.

Table 2

Test results: transport parameters of water and ethanol for  $\text{Ca}^{2+}$  cross-linked alginate magnetite membranes

	Magnetite content, w/w%					
	Water					
	0	5	10	15	20	25
Diffusion coefficient $D_L \cdot 10^{10}, \text{ cm}^2 \cdot \text{s}^{-1}$	$7.49 \pm 0.96$	$5.48 \pm 0.78$	$5.77 \pm 0.69$	$4.62 \pm 0.54$	$4.43 \pm 0.25$	$3.13 \pm 0.22$
Flux $J, \text{ g} \cdot \text{m}^{-2} \cdot \text{h}^{-1}$	$166.07 \pm 4.60$	$161.32 \pm 4.47$	$179.84 \pm 3.37$	$182.77 \pm 4.63$	$224.81 \pm 5.10$	$131.60 \pm 3.35$
Permeation coefficient $P \cdot 10^{14}, \text{ Barrer}$	$11.54 \pm 0.53$	$12.22 \pm 0.44$	$14.19 \pm 0.64$	$16.86 \pm 0.93$	$17.90 \pm 0.84$	$17.18 \pm 0.94$
Solubility coefficient $S \cdot 10^4, \text{ g} \cdot \text{cm}^{-3} \cdot \text{Pa}^{-1}$	$1.54 \pm 0.35$	$2.23 \pm 0.33$	$2.46 \pm 0.30$	$3.65 \pm 0.36$	$4.04 \pm 0.25$	$5.49 \pm 0.41$
	Ethanol					
Diffusion coefficient $D_L \cdot 10^{10}, \text{ cm}^2 \cdot \text{s}^{-1}$	$4.71 \pm 0.12$	$6.93 \pm 0.09$	$9.79 \pm 2.78$	$10.48 \pm 1.27$	$14.72 \pm 2.86$	$16.85 \pm 1.49$
Flux $J, \text{ g} \cdot \text{m}^{-2} \cdot \text{h}^{-1}$	$11.29 \pm 0.15$	$11.42 \pm 0.12$	$12.05 \pm 0.45$	$11.21 \pm 0.65$	$11.79 \pm 0.43$	$12.39 \pm 0.50$
Permeation coefficient $P \cdot 10^{14}, \text{ Barrer}$	$0.52 \pm 0.07$	$0.55 \pm 0.04$	$0.59 \pm 0.08$	$0.59 \pm 0.03$	$0.59 \pm 0.06$	$0.67 \pm 0.13$
Solubility coefficient $S \cdot 10^4, \text{ g} \cdot \text{cm}^{-3} \cdot \text{Pa}^{-1}$	$0.11 \pm 0.01$	$0.08 \pm 0.01$	$0.06 \pm 0.01$	$0.05 \pm 0.01$	$0.04 \pm 0.01$	$0.04 \pm 0.01$
Ideal selectivity $P_{\text{H}_2\text{O}}/P_{\text{EtOH}}$	$22.28 \pm 0.56$	$23.04 \pm 1.36$	$24.16 \pm 1.22$	$32.18 \pm 1.51$	$30.40 \pm 1.39$	$25.50 \pm 0.82$

### 3.3. Comparison of ethanol/water separation through different cross-linked alginate membranes filled with iron oxide magnetite nanoparticles

In both cases, the addition of iron oxide magnetic nanoparticles to the polymer matrix has a specific impact on the separation between ethanol/water mixtures. In the case of membranes cross-linked with orthophosphoric acid, the diffusion coefficients of both considered components were very similar and decreased after the addition of magnetite. For membranes cross-linked with  $\text{Ca}^{+2}$  ions, the ratio between water and ethanol diffusion coefficients conversely changed after addition of ferroferric oxide nanoparticles to polymer matrix.

In the case of water permeated both through orthophosphoric acid and  $\text{Ca}^{+2}$  cross-linked alginate membranes, higher dose of magnetite nanoparticles increased solubility coefficients. However, higher values of the solubility coefficients were obtained for alginate membranes cross-linked with orthophosphoric acid. As confirmed by the Fourier transform infrared (FTIR) method, phosphoric acid established a linkage with NaAlg through ester formation, which stabilized the chemical structure of the membrane. In orthophosphoric acid cross-linked alginate membranes, covalent interactions between phosphoric acid moieties with hydroxyl groups present in the NaAlg are responsible for the cross-linking mechanism. This interactions strengthen the charge density in alginate membranes leading to an increase in affinity of membrane towards water molecule [30]. Conversely,  $\text{Ca}^{+2}$  ions bind with  $\alpha$ -L-guluronic acid blocks resulting in the bridging of two blocks in the neighbouring alginate chains leading to the formation of 3-D water-insoluble gel network [31].  $\text{Ca}^{+2}$  cross-linked NaAlg membranes appeared more dense and rehydrated to a lesser extent in water, which have led to less favourable transport properties, especially in the case of dry cast gelation. The ethanol solubility coefficients of both types of membranes were lower than for water. NaAlg membranes have a strong affinity to water, which allows these materials to be wetted immediately. For such membranes, water rather than ethanol passes preferably through the membrane.

The results have shown that the orthophosphoric acid cross-linked alginate membranes with magnetite addition have superior separation properties to the magnetic alginate membranes cross-linked with  $\text{Ca}^{+2}$  ions. It is demonstrated by the greater difference between the received permeability

coefficients for water and ethanol and higher levels of calculated ideal selectivity coefficients (Fig. 4). The most desirable selectivity conditions were achieved for alginate membranes cross-linked with orthophosphoric acid with 5 and 10 w/w% iron oxide particles content.

## 4. Conclusions

In this paper, we have discussed the influence of two types of cross-linkers, that is, orthophosphoric acid and  $\text{Ca}^{+2}$  ions, and ferroferric oxide nanoparticles presence on the properties of NaAlg membranes. In vapour permeation experiments, the magnetic particles content ranged from 0 to 25 w/w%. Observed influence on separation properties for orthophosphoric acid cross-linked alginate membranes manifested in higher ideal selectivity coefficient that for  $\text{Ca}^{+2}$  ions cross-linked one. The addition of iron oxide nanoparticles influenced both the diffusion and solubility coefficients of water and ethanol. Comparing the separation properties on the basis of ideal selectivity coefficients, it can be concluded that the orthophosphoric acid cross-linked alginate membrane with iron oxide addition has better separation properties than the corresponding  $\text{Ca}^{+2}$  cross-linked membrane. It has been demonstrated by the greater difference between the permeability coefficient for water and ethanol. The most suitable separation parameters were obtained for membranes with 5 and 10 w/w%, and 15 and 20 w/w% for orthophosphoric acid and  $\text{Ca}^{+2}$  ions cross-linked alginate membranes, respectively. Substantial difference between flux and permeation coefficient values for the same dose of magnetite provides promising results for effective and efficient separation of ethanol/water mixture and more effective concentration process of ethanol solutions.

## Acknowledgement

The authors would like to thank Silesian University of Technology for providing financial support under the project BKM-507/RCH4/2015.

## References

- [1] U. Sander, H. Janssen, Industrial applications of vapor permeation, *J. Membr. Sci.*, 61 (1991) 113–129.
- [2] R. Rautenbach, R. Albrecht, *Membrane Processes*, Wiley, USA, 1989.
- [3] R.W. Baker, *Membrane Technology and Applications*, John Wiley & Sons, New York, USA, 2004.
- [4] R.D. Noble, S.A. Stern, *Membrane Separation Technology: Principles and Applications*, Elsevier Science Publishers, Amsterdam, The Netherlands, 1995.
- [5] A. Basile, A. Figoli, M. Khayet, *Pervaporation, Vapour Permeation and Membrane Distillation*, 1st ed., Woodhead Publishing, Elsevier, UK, USA, 2015.
- [6] R.Y.M. Huang, *Pervaporation Membrane Separation Processes*, Elsevier Science, Amsterdam, The Netherlands, 1991.
- [7] S. Ebnesajjad, *Handbook of Biopolymers and Biodegradable Plastics*, 1st ed., William Andrew, Elsevier, UK, 2012.
- [8] M. Elnashar, *Biopolymers*, Sciyo, Rijeka, Croatia, 2010.
- [9] S. Thomas, N. Ninan, S. Mohan, E. Francis, *Natural Polymers, Biopolymers, Biomaterials, and Their Composites, Blends, and IPNs*, Apple Academic Press, Toronto, New Jersey, Canada, 2013.
- [10] M. Niaounakis, *Biopolymers: Applications and Trends*, William Andrew, Elsevier, UK, 2015.

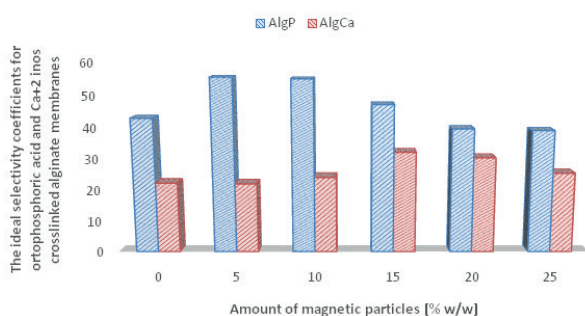


Fig. 4. The ideal selectivity coefficients for orthophosphoric acid and  $\text{Ca}^{+2}$  cross-linked alginate membranes.

- [11] D. Yang, J. Li, Z. Jiang, L. Lu, X. Chen, Chitosan/TiO<sub>2</sub> nano-composite pervaporation membranes for ethanol dehydration, *Chem. Eng. Sci.*, 64 (2009) 3130–3137.
- [12] H.G. Premakshi, K. Ramesh, M.Y. Kariduraganavar, Modification of cross-linked chitosan membrane using NaY zeolite for pervaporation separation of water–isopropanol mixtures, *Chem. Eng. Res. Des.*, 94 (2015) 32–43.
- [13] H. Sun, L. Lu, X. Chen, Z. Jiang, Pervaporation dehydration of aqueous ethanol solution using H-ZSM-5 filled chitosan membranes, *Sep. Purif. Technol.*, 58 (2008) 429–436.
- [14] Y.-L. Liu, C.-Y. Hsu, Y.-H. Su, J.-Y. Lai, Chitosan-silica complex membranes from sulfonic acid functionalized silica nanoparticles for pervaporation dehydration of ethanol–water solutions, *Biomacromolecules*, 6 (2005) 368–373.
- [15] J.G. Varghese, R.S. Karuppannan, M.Y. Kariduraganavar, Development of hybrid membranes using chitosan and silica precursors for pervaporation separation of water + isopropanol mixtures, *J. Chem. Eng. Data*, 55 (2010) 2084–2092.
- [16] G. Dudek, R. Turczyn, A. Strzelewicz, M. Krasowska, A. Rybak, Z.J. Grzywna, Studies of separation of vapours and gases through composite membranes with ferroferric oxide magnetic nanoparticles, *Sep. Purif. Technol.*, 109 (2013) 55–63.
- [17] G. Dudek, R. Turczyn, A. Strzelewicz, A. Rybak, M. Krasowska, Z.J. Grzywna, Preparation and characterization of iron oxides – polymer composite membranes, *Sep. Sci. Technol.*, 47 (2012) 1390–1394.
- [18] G. Dudek, A. Strzelewicz, R. Turczyn, M. Krasowska, A. Rybak, The study of ethanol/water vapors permeation through sulfuric acid cross-linked chitosan magnetic membranes, *Sep. Sci. Technol.*, 49 (2014) 1761–1767.
- [19] G. Dudek, M. Gnus, R. Turczyn, A. Strzelewicz, M. Krasowska, Pervaporation with chitosan membranes containing iron oxide nanoparticles, *Sep. Purif. Technol.*, 133 (2014) 8–15.
- [20] M. Gnus, G. Dudek, R. Turczyn, A. Tórz, D. Łącka, K. Konieczny, M. Łapkowski, Pervaporative investigation of ethyl alcohol dehydration, *Prog. Chem. Appl. Chitin Deriv.*, 20 (2015) 54–63.
- [21] R. Turczyn, M. Gnus, G. Dudek, A. Tórz, D. Łącka, A. Strzelewicz, M. Łapkowski, Vapour permeation study of water and ethanol through crosslinked chitosan and alginate membranes, *Prog. Chem. Appl. Chitin Deriv.*, 20 (2015) 281–288.
- [22] A. Strzelewicz, Z.J. Grzywna, Studies on the air membrane separation in the presence of a magnetic field, *J. Membr. Sci.*, 294 (2007) 60–67.
- [23] J. Crank, G. Park, *Diffusion in Polymers*, Academic Press Inc., New York and London, 1968.
- [24] B. Kruczek, H.L. Frisch, R. Chapanian, Analytical solution for the effective time lag of a membrane in a permeate tube collector in which Knudsen flow regime exists, *J. Membr. Sci.*, 256 (2005) 57–63.
- [25] S. Lashkari, B. Kruczek, Effect of resistance to gas accumulation in multi-tank receivers on membrane characterization by the time lag method. Analytical approach for optimization of the receiver, *J. Membr. Sci.*, 360 (2010) 442–453.
- [26] J. Crank, *The Mathematics of Diffusion*, Oxford University Press, 1975.
- [27] R.W. Baker, J.G. Wijmans, Y. Huang, Permeability, permeance and selectivity: a preferred way of reporting pervaporation performance data, *J. Membr. Sci.*, 348 (2010) 346–352.
- [28] F. Franks, *Water: A Matrix of Life*, Royal Society of Chemistry, UK, 2000.
- [29] S. Dixit, J. Crain, W.C.K. Poon, J.L. Finney, A.K. Soper, Molecular segregation observed in a concentrated alcohol–water solution, *Nature*, 416 (2002) 829–832.
- [30] S. Kalyani, B. Smitha, S. Sridhar, A. Krishnaiah, Pervaporation separation of ethanol–water mixtures through sodium alginate membranes, *Desalination*, 229 (2008) 68–81.
- [31] Y.J. Crossingham, P.G. Kerr, R.A. Kennedy, Comparison of selected physico-chemical properties of calcium alginate films prepared by two different methods, *Int. J. Pharm.*, 473 (2014) 259–269.